

Long-range fluctuation–induced forces in driven electrolytes

Saeed Mahdisoltani^{1,2} and Ramin Golestanian^{2,1}

¹*Rudolf Peierls Centre for Theoretical Physics, University of Oxford, Oxford OX1 3PU, United Kingdom*

²*Max Planck Institute for Dynamics and Self-Organization (MPIDS), D-37077 Göttingen, Germany*

(Dated: November 25, 2024)

We study the stochastic dynamics of an electrolyte driven by a uniform external electric field and show that it exhibits generic scale invariance despite the presence of Debye screening. The resulting long-range correlations give rise to a Casimir-like fluctuation–induced force between neutral boundaries that confine the ions, which is controlled by the electric field and can be both attractive and repulsive, unlike other known examples of fluctuation–induced forces. This work highlights the importance of nonequilibrium correlations in electrolytes and ionic liquids and how they can be used to tune interactions between uncharged structures at large separations in biological and synthetic systems.

Fluctuation–induced forces (FIFs) can arise between external objects that modify the spectrum of the fluctuations in a correlated medium, in a wide range of systems [1, 2]. While in media where fluctuations have finite correlation lengths—such as the Debye screening length in electrolytes—FIFs are finite-ranged, scale-free correlations give rise to long-ranged FIFs with universal properties [3]. Examples of such FIFs include the Casimir attraction between metallic plates due to the quantum fluctuations of the electromagnetic vacuum [4] and the forces arising from fluctuations in a critical system [5, 6]. Out of thermal equilibrium, long-range correlations are common as they may arise, e.g., from the interplay between conservation laws of the dynamics and a mismatch between fluctuations and dissipation [7–9]. Such FIFs have been investigated in a variety of nonequilibrium settings such as nonuniform temperature profiles [10], nonequilibrium diffusive dynamics [11], abrupt temperature quenches [12, 13], active systems [14], and Brownian and driven charged particles [15, 16]. Confined electrolytes and ionic liquids are highly structured fluids [17] that are ubiquitous in various areas of nanotechnology [18, 19], and in biology [20, 21]. Therefore, it is desirable to understand the mechanisms by which correlations in these systems can lead to interactions, for example in biological or synthetic nanopores (see Fig. 1).

It is well known that in thermal equilibrium, FIFs between surfaces immersed in electrolytes are short-ranged due to the screening effects of the mobile charges [22, 23]. Here, we examine the FIF arising from confining a strong electrolyte which is driven out of equilibrium by an external electric field. We show that the anisotropy introduced by the electric field gives rise to *generic scale invariance* of the dynamics [24], leading to long-ranged density and charge correlation functions. The existence of such scale-free correlations has considerable implications on the dynamics of external boundaries that enclose such a medium. Using the Maxwell stress tensor, we calculate the FIF that results from confinement of the electrolyte driven by the electric field $\mathbf{E} = E\hat{e}_x$ in the parallel-plate geometry (see Fig. 1) and find that in

d spatial dimensions the force per unit area is given as

$$\frac{F}{S} = -\frac{k_B T}{H^d} \mathcal{E}^4 \mathcal{A}(\mathcal{E}, \lambda) = -\frac{\left(\frac{\epsilon_{\text{in}}}{2S_d} E^2\right)^2}{k_B T C_0} \cdot \frac{\mathcal{A}(\mathcal{E}, \lambda)}{C_0 H^d}, \quad (1)$$

where H is the separation between the plates. The above result depends on the dimensionless electric field \mathcal{E} , which represents the ratio between the electric field (Maxwell) stress and the osmotic pressure of the electrolyte, and the dielectric contrast λ that are defined as follows

$$\mathcal{E} = \left[\frac{\epsilon_{\text{in}} E^2}{2S_d k_B T C_0} \right]^{1/2}, \quad \text{and} \quad \lambda = \frac{\epsilon_{\text{in}} - \epsilon_{\text{out}}}{\epsilon_{\text{in}} + \epsilon_{\text{out}}}. \quad (2)$$

Here, ϵ_{in} and ϵ_{out} represent the dielectric constants of the electrolyte and the boundaries, respectively, C_0 is the mean concentration (of each charge type) in the electrolyte, and $S_d = 2\pi^{d/2}/\Gamma(d/2)$ is the area of d -dimensional unit sphere. The dimensionless amplitude $\mathcal{A}(\mathcal{E}, \lambda)$ is a constant for $\mathcal{E} \ll 1$, which shows that the FIF scales as $\sim E^4$ for relatively weak electric fields, whereas for $\mathcal{E} \gg 1$ it behaves as $\mathcal{A} \sim 1/\mathcal{E}^2$ (see Table. I), which shows that for large applied electric fields

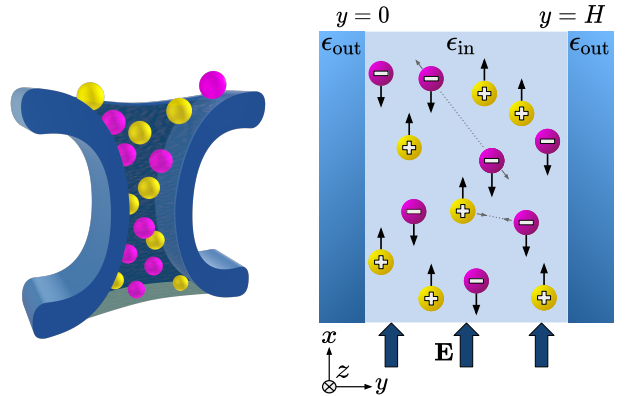


FIG. 1. Schematics of an ion channel (left) and the driven electrolyte model in flat geometry (right). The external electric field $\mathbf{E} = E\hat{e}_x$ drives the positive and negative charges in opposite directions (black arrows) and, in addition, the charges exert electrostatic forces on each other (gray arrows).

the force is $\sim E^2$. Intriguingly, the amplitude \mathcal{A} varies non-monotonically with both \mathcal{E} , and it can change sign (see Fig. 2). This indicates that the resulting FIF can be tuned to be both repulsive and attractive in the same setup, which is a feature that has not been previously observed in Casimir-like interactions.

Stochastic Density Equations— We consider a symmetric collection of charged particles with charges $\pm Q$ and with equal mobilities $\mu_+ = \mu_- = \mu$ that undergo Brownian motion as a result of the microscopic collisions with the implicit solvent molecules (the hydrodynamic effects of the solvent are neglected throughout this work). In the overdamped regime, the trajectory of a (positively- or negatively-) charged particle labeled a is described by the Langevin dynamics

$$\dot{\mathbf{r}}_a^\pm(t) = \mu(\pm Q) [-\nabla\phi(\mathbf{r}_a^\pm(t)) + \mathbf{E}] + \sqrt{2D}\boldsymbol{\eta}_a^\pm(t), \quad (3)$$

where ϕ is the electrostatic potential created by the charged particles, and $\boldsymbol{\eta}_a^\pm$ represent independent Gaussian white noises characterized by $\langle \eta_{ai}^\pm(t)\eta_{bj}^\pm(t') \rangle = \delta_{ab}\delta_{ij}\delta(t-t')$ and zero mean. At this microscopic level, the fluctuation-dissipation relation connects the noise strength D to the mobility μ through the Einstein relation $\mu = \beta D$, where $\beta = 1/(k_B T)$ represents the inverse temperature of the system.

Using the instantaneous number density of each type of charge, which is defined as $C^\pm(\mathbf{r}, t) = \sum_a \delta^d(\mathbf{r} - \mathbf{r}_a^\pm(t))$, one can express the electrostatic Poisson equation in Gaussian units as $-\nabla^2\phi = S_d Q(C^+ - C^-)/\epsilon_{\text{in}}$. Using the Dean-Kawasaki approach [25–27], the dynamics of C^\pm can be obtained exactly as continuity equations, i.e. $\partial_t C^\pm + \nabla \cdot \mathbf{J}^\pm = 0$, where the stochastic currents are given by $\mathbf{J}^\pm = -D\nabla C^\pm \pm \mu C^\pm Q(-\nabla\phi + \mathbf{E}) - \sqrt{2DC^\pm}\boldsymbol{\eta}^\pm$. Here, $\boldsymbol{\eta}^\pm$ are uncorrelated Gaussian noise fields characterized by zero averages and $\langle \eta_i^\pm(\mathbf{r}, t)\eta_j^\pm(\mathbf{r}', t') \rangle = \delta_{ij}\delta^d(\mathbf{r} - \mathbf{r}')\delta(t - t')$.

The Dean-Kawasaki equations for C^\pm are analytically intractable due to the nonlinear terms (i.e., $C^\pm \nabla\phi$) as well as the multiplicative noise. To avoid these difficulties, we consider the dynamics of the density and charge fluctuations around a state with uniform distribution of the particles, which allows us to linearize the density equations. This simplification remains valid for a dense population of soft particles [28] and has been used, e.g., to study the conductivity of strong electrolytes [29], fluctuations of ionic currents across nanopores [30, 31], and driven binary mixtures [32]. We have also examined the scaling behavior of the nonlinear terms which reveals that they are irrelevant at the macroscopic level (see Ref. [33] for details). We therefore write the density of each type of charge as $C^\pm = C_0 + \delta C^\pm$ and assume the density fluctuations δC^\pm are small compared to the background C_0 , i.e., $\delta C^\pm \ll C_0$. Defining the (total) number density fluctuations $c(\mathbf{r}, t) = \delta C^+ + \delta C^-$ and the charge density fluctuations $\rho(\mathbf{r}, t) = \delta C^+ - \delta C^-$ (in units of Q), the

linearized stochastic equations of δC^\pm can be recast as

$$\partial_t c = D\nabla^2 c - \mu Q \mathbf{E} \cdot \nabla \rho + \sqrt{4DC_0}\eta_c, \quad (4)$$

$$\partial_t \rho = D\nabla^2 \rho - \mu Q \mathbf{E} \cdot \nabla c - D\kappa^2 \rho + \sqrt{4DC_0}\eta_\rho. \quad (5)$$

Here the Debye screening length κ^{-1} is defined through $\kappa^2 = 2S_d C_0 \ell_B$ with the ‘‘Bjerrum length’’ $\ell_B = \beta Q^2 / \epsilon_{\text{in}}$ (in d spatial dimensions $\ell_B \sim (\text{length})^{d-2}$). In addition, the linearized noise correlations are given as $\langle \eta_\rho(\mathbf{r}, t)\eta_\rho(\mathbf{r}', t') \rangle = \langle \eta_c(\mathbf{r}, t)\eta_c(\mathbf{r}', t') \rangle = -\nabla^2 \delta^d(\mathbf{r} - \mathbf{r}')\delta(t - t')$, and η_ρ and η_c have zero averages and are uncorrelated.

In the absence of the external electric field ($\mathcal{E} = 0$), Eqs. (4) and (5) describe the usual diffusion of the number density c , together with the relaxation of the charge density ρ with the Debye relaxation time $(D\kappa^2)^{-1}$. In the presence of the electric field, however, these dynamics become nontrivial due to the coupling through the electric field between ρ and c ; this coupling introduces a charge contribution that persists beyond the Debye relaxation time. Focusing on the dynamics of the particles beyond the Debye length- and time-scale κ^{-1} and $(D\kappa^2)^{-1}$ allows for a quasi-stationary solution for ρ which reads

$$\rho \approx -\kappa^{-2} \beta Q \mathbf{E} \cdot \nabla c, \quad (6)$$

where we have made use of the Einstein relation. The Debye length for typical electrolyte solutions is of the order of $\kappa^{-1} \sim 1 - 10$ nm [34] and therefore this approximation applies to boundary separations beyond this scale, e.g., in the case of wet ion channels such as mechanosensitive channels [21] and synthetic nanopores [18].

Substituting Eq. (6) back into Eq. (5), we obtain an *anisotropic* diffusion equation for c that reads

$$\partial_t c = D(\mathcal{E}^2 \partial_x^2 + \nabla^2)c + \sqrt{4DC_0}\eta_c, \quad (7)$$

where the dimensionless electric field \mathcal{E} is defined in Eq. (2) and, alternatively, can be expressed in terms of the Debye length as $\mathcal{E} = \beta Q \mathbf{E} / \kappa$. Note that we have discarded the noise η_ρ when substituting Eq. (6) into Eq. (4) since it is negligible with respect to η_c due to the presence of an additional gradient operator. It is worth mentioning that although the Einstein relation was assumed between the mobility and the noise strength in the microscopic Langevin equation (3), a similar relation does not hold anymore at the macroscopic level of Eq. (7). As a result of this mismatch between the noisy fluctuations and the dissipative forces in the conserved dynamics, the dynamics of c represents a realization of generic scale invariance [7, 8], i.e., it automatically gives rise to long-ranged correlations without a tuning parameter.

Correlation Functions— The steady-state bulk correlation functions can be readily obtained through Fourier transformations by making use of the translational invariance of the dynamics. Defining $\langle c(\mathbf{k}, t)c(\mathbf{k}', t) \rangle \equiv$

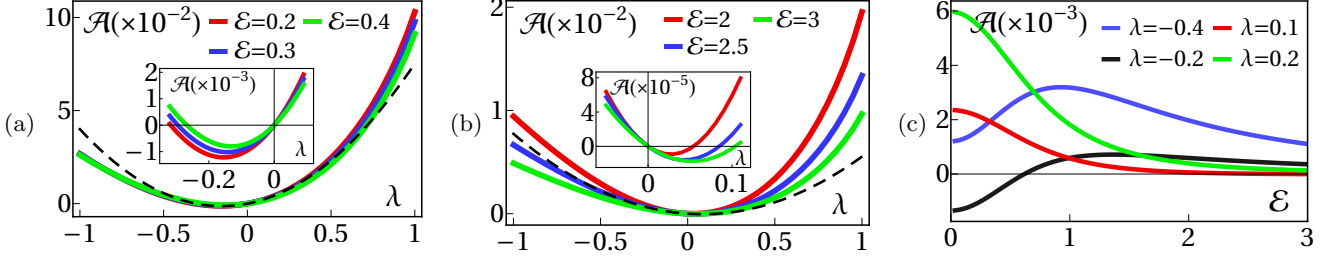


FIG. 2. The FIF amplitude \mathcal{A} calculated from Eq. (11) as a function of λ for small applied electric fields (a) and large electric fields (b), and as a function of \mathcal{E} for various values of λ (c). The solid lines are obtained from exact numerical computation of Eq. (11), while the dashed lines in (a) and (b) are, respectively, the approximate forms for $\mathcal{E} \ll 1$ (which is independent of \mathcal{E}) and $\mathcal{E} \gg 1$ (computed for $\mathcal{E} = 3$). Analysing the asymptotic expressions given in Table. I reveals three distinct behaviors of \mathcal{A} as a function of \mathcal{E} (panel c): for $-0.3 \lesssim \lambda < 0$, the amplitude \mathcal{A} starts from a negative value, crosses to positive values and falls off to zero for large \mathcal{E} ; for $0 < \lambda \lesssim 0.16$, the amplitude \mathcal{A} initially starts from positive values, crosses to negative values before approaching zero from below for large \mathcal{E} ; and, finally, for $\lambda \lesssim -0.3$ or $\lambda \gtrsim 0.16$, \mathcal{A} remains positive when changing \mathcal{E} .

$\langle c(\mathbf{k})c(\mathbf{k}') \rangle \equiv (2\pi)^d \delta^d(\mathbf{k} + \mathbf{k}') [2C_0 + c_{\text{bulk}}^{(2)}(\mathbf{k})]$, we obtain

$$c_{\text{bulk}}^{(2)}(\mathbf{k}) = -\frac{2C_0 \mathcal{E}^2 k_x^2}{(\mathcal{E}^2 + 1)(k_x^2 + k_y^2 + k_z^2)}. \quad (8)$$

which is the nonequilibrium correlation due to the external electric field (it vanishes for $\mathcal{E} = 0$), with the anisotropy rendering the $\mathbf{k} \rightarrow 0$ singular (depending on the order of the limit for the different components). In real space, we obtain (in the steady-state)

$$c_{\text{bulk}}^{(2)}(\mathbf{r}) = -\frac{2C_0 \mathcal{E}^2}{S_d (\mathcal{E}^2 + 1)^{3/2}} \frac{(1-d)\tilde{x}^2 + y^2 + z^2}{(\tilde{x}^2 + y^2 + z^2)^{1+d/2}}, \quad (9)$$

where $\tilde{x} = x/\sqrt{\mathcal{E}^2 + 1}$. This expression clearly displays the anisotropy in the correlation functions and shows that in d dimensions, the density correlations decrease as $\sim r^{-d}$ with distance. The charge correlations in the bulk can be obtained from Eq. (9) by making use of the relation (6). It is therefore seen that the charge fluctuations are also long-range correlated in the bulk.

We now calculate the steady-state correlation functions in the presence of boundaries. As depicted in Fig. 1, we consider a plane parallel geometry with boundaries located at $y = 0$ and $y = H$. The walls are assumed impenetrable and as such correspond to no-flux Neumann boundary conditions. With these Neumann boundary conditions, the solutions of Eq. (7) can be constructed through decomposing c and η_c onto the cosine modes $\cos(p_n y)$ where $p_n = \frac{n\pi}{H}$ [12, 35]. This leads to the discretized form of Eq. (8), viz

$$c^{(2)}(y, y'; k_x, \mathbf{k}_z) = \frac{-4C_0 k_x^2 \mathcal{E}^2}{H} \sum_{n=0}^{\infty} \frac{\cos(p_n y) \cos(p_n y')}{(\mathcal{E}^2 + 1)(k_x^2 + p_n^2 + \mathbf{k}_z^2)},$$

where we now have $\langle c(y; k_x, \mathbf{k}_z) c(y'; k'_x, \mathbf{k}'_z) \rangle = (2\pi)^{d-1} \delta(k_x + k'_x) \delta^{d-2}(\mathbf{k}_z + \mathbf{k}'_z) [2C_0 \delta(y - y') + c^{(2)}(y, y'; k_x, \mathbf{k}_z)]$ and \sum' means the $n = 0$ term takes an additional factor of $1/2$. By making use of

Eq. (6), the charge fluctuations are then obtained as

$$\rho^{(2)}(y, y'; k_x, \mathbf{k}_z) = \frac{2C_0 k_x^2 \mathcal{E}^2}{\kappa^2} \delta(y - y') - \frac{4C_0 k_x^4 \mathcal{E}^4}{\kappa^2 H} \sum_{n=0}^{\infty} \frac{\cos(p_n y) \cos(p_n y')}{(\mathcal{E}^2 + 1)(k_x^2 + p_n^2 + \mathbf{k}_z^2)}, \quad (10)$$

where $\rho^{(2)}$ is defined similarly to $c^{(2)}$. Note that due to the screening effect, only nonequilibrium contributions to the charge correlations survive in this regime (see details in Ref. [33]) and as such the r.h.s of Eq. (10) vanishes when $\mathcal{E} = 0$. Lastly, we note that the local contribution $\propto k_x^2 \delta(y - y')$ in the charge correlation function is an artifact of the uniform background density C_0 of the particles (see Ref. [33]), which does not contribute to the forces on the boundaries. Therefore, this term shall be discarded when calculating the stress tensor.

Stress Tensor— The nonequilibrium pressure exerted on the boundaries located at $y = 0$ and H can be calculated via the noise-averaged Maxwell stress $\langle \sigma_{ij} \rangle = \frac{\epsilon_{\text{in}}}{2S_d} (2\langle \nabla_i \phi \nabla_j \phi \rangle - \delta_{ij} \langle (\nabla \phi)^2 \rangle)$ [36]. We assume no free charges on the boundaries, and the electrostatic boundary conditions are given by $\epsilon_{\text{in}} \partial_y \phi|_{y=0^+, H^-} = \epsilon_{\text{out}} \partial_y \phi|_{y=0^-, H^+}$ and the continuity of the parallel derivatives. The electric potential satisfying these conditions can be obtained using the method of images [37] and reads as $\phi(\mathbf{r}) = \sum_{n \in \mathbb{Z}} \int_{\mathbf{r}'} (\lambda^n \rho(\mathbf{r}') Q) / (\epsilon_{\text{in}} (d-2) |\mathbf{r} - \mathbf{r}'_n|^{d-2})$ where n indexes the image charges located at $\mathbf{r}'_n = (x', 2nH \pm y', z')$ and λ [as defined in Eq. (2)] represents the ratio of the successive image charges. Upon substituting $\phi(\mathbf{r})$ into the Maxwell stress, performing the summation over the image charges, and using Eq. (10), we arrive at Eq. (1) for the normal force on the boundary at $y = H$ where the amplitude is given by [33]

$$\mathcal{A}(\mathcal{E}, \lambda) = \int_{\nu} \sum_{n=0}^{\infty} \frac{2^{1-d} \nu_x^4 \nu^2 \mathcal{R}_n(\lambda, \nu)}{(\mathcal{E}^2 \nu_x^2 + n^2 + \nu^2)(n^2 + \nu^2)^2}, \quad (11)$$

and we have defined

$$\mathcal{R}_n(\lambda, \nu) = \lambda \frac{(e^{2\pi\nu} - \lambda + (-1)^n(\lambda - 1)e^{\pi\nu})^2}{(e^{2\pi\nu} - \lambda^2)^2} - \lambda, \quad (12)$$

with the dimensionless momentum $\boldsymbol{\nu} = (\nu_x, \nu_z) \in \mathbb{R}^{d-1}$ and $\nu = \sqrt{\nu_x^2 + \nu_z^2}$ (the force exerted on the $y = 0$ boundary has the same magnitude and is in the opposite direction). Figure 2 shows the variation of \mathcal{A} as a function of λ [Fig. 2(a) and Fig. 2(b)] and \mathcal{E} [Fig. 2(c)], for the $d = 3$ dimensional case, obtained numerically from Eq. (11). In Table I, we also summarize the approximate forms for \mathcal{A} in $d = 3$ which are obtained from the suitable asymptotic expansion of Eq. (11) in each regime. These approximate forms are shown in Fig. 2(a) and Fig. 2(b) as dashed lines.

From Eq. (11) and the asymptotic forms in Table I, we note that the FIF exhibits two different regimes for weak and strong applied electric fields: for weak electric fields ($\mathcal{E} \ll 1$), the force scales as E^4 and is proportional to the inverse temperature ($\propto \beta$) and the inverse of the square of the average number density ($\propto 1/C_0^2$); for strong electric fields ($\mathcal{E} \gg 1$), on the other hand, the force scales as E^2 with the electric field, is independent of temperature and proportional to the inverse of the average number density ($\propto 1/C_0$). Fig. 2 also shows that the sign of the force amplitude can change with the applied electric field: for $\lambda \ll 1$ (i.e. small dielectric contrast between the electrolyte and the plates), the amplitude \mathcal{A} can become negative which, remarkably, indicates a repulsive fluctuation-induced force between boundaries that enclose the driven electrolyte. For moderate values of the dielectric contrast λ , on the other hand, the force amplitude remains positive, representing an attraction between the boundaries.

Concluding Remarks— In this work, we showed that the steady-state density and charge fluctuations in a driven electrolyte are long-range correlated as a result of the effective anisotropy introduced by the external electric field. These nonequilibrium fluctuations give rise to long-range FIFs on external objects and boundaries immersed in the driven electrolyte. The resulting normal force per unit area on the boundaries varies non-monotonically with the electric field and the dielectric contrast, and, remarkably, can be tuned to be attractive or repulsive with different amplitudes by varying the relevant parameters. We note that the setup here gives an independent mechanism for tuning nonequilibrium FIFs from the one introduced in Ref. [16] and investigating the interplay of the two effects forms an interesting direction for future studies.

It is worth mentioning that long-ranged forces have recently been observed in electrolytes in a number of experimental settings [38–40] where oscillatory (AC) electric fields are applied to charged solutions. In future works, we plan to extend our analysis to investigate the nonequi-

	$\mathcal{E} \ll 1$	$\mathcal{E} \gg 1$
$\lambda \ll 1$	$\frac{9(4\zeta(5)+1)}{256\pi}\lambda^2 + \frac{9(4\zeta(5)-1)}{512\pi}\lambda$	$\frac{\lambda(6\lambda-1)}{32\pi}\mathcal{E}^{-2}$
$\lambda = 1$	$\frac{9\zeta(3)}{32\pi}$	$\frac{\zeta(3)}{4\pi}\mathcal{E}^{-2}$
$\lambda = -1$	$\frac{9\zeta(3)}{128\pi}$	$\frac{\zeta(3)}{8\pi}\mathcal{E}^{-2}$

TABLE I. Leading order approximations of the stress amplitude $\mathcal{A}(\mathcal{E}, \lambda)$ in $d = 3$ obtained from expanding Eq. (11). (corrections are $\mathcal{O}(\mathcal{E}^2)$ for $\mathcal{E} \ll 1$, and $\mathcal{O}(\mathcal{E}^{-4})$ for $\mathcal{E} \gg 1$). The values of the Riemann zeta function here are $\zeta(5) \approx 1.04$ and $\zeta(3) \approx 1.20$.

librium FIF in an electrolyte in the presence of a time-varying electric field. Finally, the model used here relies on the linearization of the stochastic dynamics which is applicable to strong electrolytes [29]. We plan to perform a more rigorous treatment of the nonlinearities using renormalization group (RG) techniques which have recently been applied to similar dynamics in the context of chemotaxis [41].

Acknowledgments – S.M. acknowledges the support of the University of Oxford Clarendon Fund Scholarships. This work was supported by the Max Planck Society.

-
- [1] Mehran Kardar and Ramin Golestanian, “The “friction” of vacuum, and other fluctuation-induced forces,” *Rev. Mod. Phys.* **71**, 1233–1245 (1999).
 - [2] Andrea Gambassi, “The Casimir effect: From quantum to critical fluctuations,” *J. Phys.: Conf. Ser.* **161**, 012037 (2009).
 - [3] Roger H. French, V. Adrian Parsegian, Rudolf Podgornik, Rick F. Rajter, Anand Jagota, Jian Luo, Dilip Asthagiri, Manoj K. Chaudhury, Yet-ming Chiang, Steve Granick, Sergei Kalinin, Mehran Kardar, Roland Kjellander, David C. Langreth, Jennifer Lewis, Steve Lustig, David Wesolowski, John S. Wettlaufer, Wai-Yim Ching, Mike Finnis, Frank Houlihan, O. Anatole von Lilienfeld, Carel Jan van Oss, and Thomas Zemb, “Long range interactions in nanoscale science,” *Rev. Mod. Phys.* **82**, 1887–1944 (2010).
 - [4] Hendrick BG Casimir, “On the attraction between two perfectly conducting plates,” *Proc. Kon. Ned. Akad. Wet.* **51**, 793 (1948).
 - [5] Michael E Fisher and PGD Gennes, “Wall phenomena in a critical binary mixture,” *C. R. Acad. Sc. Paris B* **287**, 207–209 (1978).
 - [6] Christopher Hertlein, Laurent Helden, Andrea Gambassi, Siegfried Dietrich, and Clemens Bechinger, “Direct measurement of critical Casimir forces,” *Nature* **451**, 172–175 (2008).
 - [7] Pedro L Garrido, Joel L Lebowitz, Christian Maes, and Herbert Spohn, “Long-range correlations for conservative dynamics,” *Phys. Rev. A* **42**, 1954 (1990).

- [8] G Grinstein, D-H Lee, and Subir Sachdev, “Conservation laws, anisotropy, and “self-organized criticality” in noisy nonequilibrium systems,” *Phys. Rev. Lett.* **64**, 1927 (1990).
- [9] Terence Hwa and Mehran Kardar, “Dissipative transport in open systems: An investigation of self-organized criticality,” *Phys. Rev. Lett.* **62**, 1813 (1989).
- [10] A Najafi and R Golestanian, “Forces induced by nonequilibrium fluctuations: The Soret-Casimir effect,” *EPL* **68**, 776–782 (2004).
- [11] Avi Aminov, Yariv Kafri, and Mehran Kardar, “Fluctuation-induced forces in nonequilibrium diffusive dynamics,” *Phys. Rev. Lett.* **114**, 230602 (2015).
- [12] Christian M Rohwer, Mehran Kardar, and Matthias Krüger, “Transient casimir forces from quenches in thermal and active matter,” *Phys. Rev. Lett.* **118**, 015702 (2017).
- [13] Christian M. Rohwer, Alexandre Solon, Mehran Kardar, and Matthias Krüger, “Nonequilibrium forces following quenches in active and thermal matter,” *Phys. Rev. E* **97**, 032125 (2018).
- [14] D. Ray, C. Reichhardt, and C. J. Olson Reichhardt, “Casimir effect in active matter systems,” *Phys. Rev. E* **90**, 013019 (2014).
- [15] David S. Dean and Rudolf Podgornik, “Relaxation of the thermal Casimir force between net neutral plates containing Brownian charges,” *Phys. Rev. E* **89**, 032117 (2014).
- [16] David S. Dean, Bing-Sui Lu, A. C. Maggs, and Rudolf Podgornik, “Nonequilibrium Tuning of the Thermal Casimir Effect,” *Phys. Rev. Lett.* **116**, 240602 (2016).
- [17] Susan Perkin, “Ionic liquids in confined geometries,” *Physical Chemistry Chemical Physics* **14**, 5052 (2012).
- [18] Z. Siwy and A. Fuliński, “Fabrication of a synthetic nanopore ion pump,” *Phys. Rev. Lett.* **89**, 198103 (2002).
- [19] Reto B Schoch, Jongyoon Han, and Philippe Renaud, “Transport phenomena in nanofluidics,” *Rev. Mod. Phys.* **80**, 839 (2008).
- [20] David J Aidley and Peter R Stanfield, *Ion channels: molecules in action* (Cambridge University Press, 1996).
- [21] B. Martinac, “Mechanosensitive ion channels: molecules of mechanotransduction,” *Journal of Cell Science* **117**, 2449–2460 (2004).
- [22] B Jancovici and L Šamaj, “Screening of classical Casimir forces by electrolytes in semi-infinite geometries,” *J. Stat. Mech.: Theory Exp.* **2004**, P08006 (2004).
- [23] Alpha A Lee, Jean-Pierre Hansen, Olivier Bernard, and Benjamin Rotenberg, “Casimir force in dense confined electrolytes,” *Mol. Phys.* **116**, 3147–3153 (2018).
- [24] G Grinstein, “Generic scale invariance in classical nonequilibrium systems,” *J. Appl. Phys.* **69**, 5441–5446 (1991).
- [25] David S Dean, “Langevin equation for the density of a system of interacting Langevin processes,” *J. Phys. A* **29**, L613 (1996).
- [26] Kyozi Kawasaki, “Stochastic model of slow dynamics in supercooled liquids and dense colloidal suspensions,” *Physica A* **208**, 35–64 (1994).
- [27] Michael te Vrugt, Hartmut Löwen, and Raphael Wittkowski, “Classical dynamical density functional theory: from fundamentals to applications,” arXiv:2009.07977 (2020).
- [28] Vincent Démery, Olivier Bénichou, and Hugo Jacquin, “Generalized Langevin equations for a driven tracer in dense soft colloids: construction and applications,” *New J. Phys.* **16**, 053032 (2014).
- [29] Vincent Démery and David S Dean, “The conductivity of strong electrolytes from stochastic density functional theory,” *J. Stat. Mech.: Theory Exp.* **2016**, 023106 (2016).
- [30] Mira Zorkot, Ramin Golestanian, and Douwe Jan Bonthuis, “The power spectrum of ionic nanopore currents: the role of ion correlations,” *Nano Lett.* **16**, 2205–2212 (2016).
- [31] Mira Zorkot and Ramin Golestanian, “Current fluctuations across a nano-pore,” *J. Phys. Condens. Matter* **30**, 134001 (2018).
- [32] Alexis Poncet, Olivier Bénichou, Vincent Démery, and Gleb Oshanin, “Universal long ranged correlations in driven binary mixtures,” *Phys. Rev. Lett.* **118**, 118002 (2017).
- [33] See Supplemental Material at [URL will be inserted by publisher] which contains more details on the scaling analysis, correlation functions, and the calculation and analysis of the stress tensor.
- [34] Jacob N Israelachvili, *Intermolecular and surface forces* (Academic press, 2011).
- [35] György Barton and Gabriel Barton, *Elements of Green’s functions and propagation: potentials, diffusion, and waves* (Oxford University Press, 1989).
- [36] Note that the construction of Maxwell stress from the electrostatic force density $\nabla \cdot \sigma = -\rho \nabla \phi$ [42] is similar to the derivation of the Irving–Kirkwood formula [43, 44], and therefore it is the appropriate stress for calculating the nonequilibrium forces.
- [37] John David Jackson, *Classical Electrodynamics* (John Wiley & Sons, 2007).
- [38] SMH Hashemi Amrei, Scott C Bukosky, Sean P Rader, William D Ristenpart, and Gregory H Miller, “Oscillating electric fields in liquids create a long-range steady field,” *Phys. Rev. Lett.* **121**, 185504 (2018).
- [39] Carla Sofia Perez-Martinez and Susan Perkin, “Surface forces generated by the action of electric fields across liquid films,” *Soft Matter* **15**, 4255–4265 (2019).
- [40] Lukasz Richter, Paweł J. Żuk, Piotr Szymczak, Jan Paczesny, Krzysztof M. Bkac, Tomasz Szymborski, Piotr Garstecki, Howard A. Stone, Robert Holyst, and Carlos Drummond, “Ions in an ac electric field: Strong long-range repulsion between oppositely charged surfaces,” *Phys. Rev. Lett.* **125**, 056001 (2020).
- [41] Saeed Mahdisoltani, Riccardo Ben Ali Zinati, Charlie Duclut, Andrea Gambassi, and Ramin Golestanian, “Quorum effects in chemotaxis: anomalous diffusion and non-Poissonian number fluctuations with exact exponents,” arXiv:1911.08115 (2020).
- [42] Herbert H Woodson and James R Melcher, *Electromechanical dynamics* (Wiley, 1968).
- [43] JH Irving and John G Kirkwood, “The statistical mechanical theory of transport processes. IV. The equations of hydrodynamics,” *J. Chem. Phys.* **18**, 817–829 (1950).
- [44] Matthias Krüger, Alexandre Solon, Vincent Démery, Christian M Rohwer, and David S Dean, “Stresses in non-equilibrium fluids: Exact formulation and coarse-grained theory,” *J. Chem. Phys.* **148**, 084503 (2018).